RSC Advances

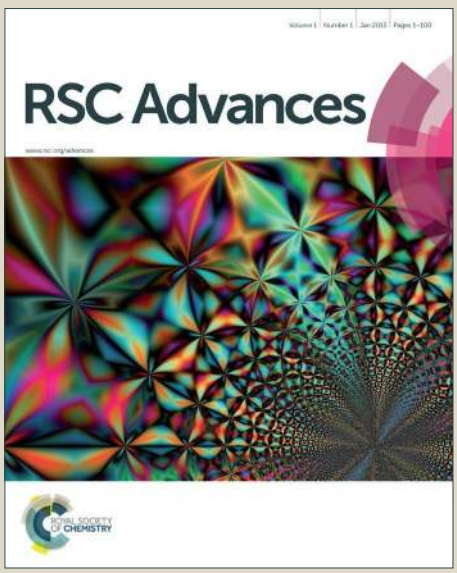

ROYAL SOCIETY OF CHEMISTRY

www.rsc.org/advances

View Article Online
DOI: 10.1039/C6RA14277J

Journal Name

ARTICLE

Outstanding electromagnetic interference shielding effectiveness of polyvinylbutyral - polyaniline nanocomposite film

Received 00th January 20xx,
Accepted 00th January 20xx

DOI: 10.1039/x0xx00000x

www.rsc.org/

Pritom J Bora[a], Gaurav Lakhani[b], Praveen C Ramamurthy[a, b*] and Giridhar Madras[a]

In this work, we have studied the electromagnetic interference (EMI) shielding property of solution processed polyvinylbutyral–polyaniline nanocomposite (PVBPN) film in the X-band (8.2-12.4 GHz) and Ku-band (12.4-18 GHz) frequency. The polyaniline nanofibers were chemically synthesized at -30±2 °C and characterized by various techniques. The optimally prepared, free standing PVBPN film (sandwiched 0.78±0.02 mm) shows an outstanding EMI shielding effectiveness in the X-band and Ku-band frequency. In the X-band, ~ 26 dB EMI shielding effectiveness (shielding due to absorption SE_A ~ 21 dB and shielding due to reflection SE_R ~ 5 dB) was obtained which was found to increase ~ 30 dB (SE_A is ~ 26 dB and SE_R ~ 4 dB) for Ku-band. The enhancement of shield conductivity, dielectric loss and EM attenuation constant with frequency results in excellent EMI shielding property of PVBPN film.

1. Introduction

At present, due to the prospective applications of electrical /electronics, the electromagnetic interference (EMI) shielding materials is most demanding especially for high frequency range (8.2-18 GHz).[1-5] The electromagnetic interference shielding by a material for an incident plane wave i.e. radiated electromagnetic wave in the far field of the source is equal to the EMI attenuation due to absorption, reflection and multiple reflections (correction factor/scattering loss).[3-5] Thus the total EMI shielding effectiveness is expressed as,

$$SE_T = SE_A + SE_R + SE_M$$

Here, SE_A, SE_R and SE_M correspond to EMI shielding effectiveness due to absorption, reflection and multiple reflections respectively. The contribution of SE_M can be neglected if SE_A is ~ 10 dB (30 dB shielding effectiveness refers 99.9 % shielding).[3, 6] For far field source, the factors which strongly effect on EMI shielding are conductivity, permeability-permittivity, dielectric loss, skin depth, EM attenuation constant and design parameter includes thickness and shield to source distance.[3, 7]

Lightweight, flexible polymer nanocomposite materials has been a key interest for EMI shielding and microwave absorption due to many advantages over traditionally used metal sheets.[3-8] Intrinsic conducting polymers (ICPs) such as polyacetylene (PA), polypyrol (PPY), polyaniline (PANI) are well known for EMI shielding.[9] Among them, PANI has drawn special attention due to its bulk level easy synthesis, tunable conductivity and molecular weight.[9-12] The electrical conductivity of PANI depends on its molecular weight and synthesizing temperature. Low temperature synthesis (~ -30 °C) has been proposed for high molecular weight PANI and hence for higher conductivity.[12] However, the electrical conductivity of polyaniline decreases with time due to de-doping.[10] It has been shown PANI in non-conducting polymer matrix shows better stability with EMI shielding.[13-15] Lakshmi *et al.* reported the EMI shielding behaviour of PU-PANI composite in S-band and X-band frequency.[13] According to their result, 1.9 mm thicker PU-

[a] Interdisciplinary Centre for Energy Research (ICER)
[b] Department of Materials Engineering
[c] Indian Institute of Science (IISc), Bangalore-560012, India
† Footnotes relating to the title and/or authors should appear here.
Electronic Supplementary Information (ESI) available: [details of any supplementary information available should be included here]. See DOI: 10.1039/x0xx00000x

View Article Online
DOI: 10.1039/C6RA14277J

PANI (PU: aniline ratio was 1:1) composite shows maximum ~ 26.7 dB shielding effectiveness at 8.8 GHz. However, the average SE is ~ 10 dB in the frequency range 8-12 GHz.[13] Similarly, Sudha *et al.* reported 16.2 dB SE of 10 weight% PANI clay loaded polystyrene (PS) composite (1 mm thickness) at the frequency 8 GHz.[14] Saini *et al*. studied the EMI shielding behaviour of PANI-multiwall CNT-PS nanocomposite.[15] Their study shows ~ 24 dB SE of 30 weight % PANI-multiwall CNT loaded PS nanocomposite (thickness 1 mm) in the frequency range 12.4-18 GHz. While thickness was increased to 2 mm, the SE_T value reached 40-45 dB.[15]

The anisotropic nanoparticles, especially group of nanofibers or nano tree structures having high dielectric loss is reported as a better microwave absorber compared to other nanostructures.[16] Mechanistically, they act like a receiver antenna which transforms electromagnetic radiation (EM energy) to micro current which propagates through the material.[16] Hence, it loses energy through dissipation current and shows high microwave absorption. Recent investigations shows PANI nanofibers exhibit some interesting behaviours and has been proposed for many potential applications including biocompatibility,[17] sensors,[18] EMI shielding[19] as well as for heat conduction.[20]

Polyvinylbutyral (PVB), a novel polymer, recently has drawn much attraction for encapsulation especially in organic electronics due to its unique moisture resistive and dielectric properties.[20-21] Hence, PVB- PANI nanofiber composite film can be expected as a potential polymer nanocomposite to coat small modern communication devices to protect against EMI. To the best of our knowledge, EMI shielding property of PVB-PANI nanofiber composite film is not reported. The objective of the present work is the synthesis of PANI nanofiberes at low temperature, preparation of PVB-PANI nanofiber composite film and investigation of EMI shielding property.

2. Experimental

2.1. Synthesis and film preparation

The PANI nanofibers were synthesized by oxidative polymerization of aniline (double distilled) at -30±2 °C in acidic aqueous (HCl)-organic (chloroform) two phase system, according to the procedure described in the literature.[23] The commercially available PVB (4 g) was dissolved in 30 ml ethanol and optimally 1.15 g of as synthesized PANI nanofiberes was added slowly to the PVB solution and further kept for stirring for another 2 h. It was then poured to a polyethylene terephthalate (PET) mould and kept for air drying (12 h). Obtained PVB-PANI nanocomposite film was named as PVBPN film. Three films were sandwiched for EMI shielding measurements and the thickness was found 0.78±0.02 mm.

2.2. Characterization and EMI shielding measurement

The surface morphologies of the synthesized PANI nanofiberes were analysed using high resolution FESEM (Carl Zeiss). The UV-visible spectra of polyaniline nanofiber were obtained by Perkin spectrophotometer. The X-ray diffractrogram was obtained through Rigaku X-ray diffractometer using Cu Kα radiation (λ=1.540598 Å) in scattering range (2θ) of 10-80°. The EMI shielding effectiveness was measured by using a vector network analyser (VNA, Agilent NS201). The scattering parameters (*S*-parameters, S_{21} and S_{11}) were determined by waveguide method after performing standard thru-reflect-line (TRL) calibration of VNA for X-band (8.2-12.4 GHz) and Ku-band (12.4-18 GHz). The complex *S*-parameters (S_{21} and S_{11}) of three sample films were measured for each frequency band. The EMI shielding effectiveness in dB is equal to $|S_{21}|$.[24] The reflectance (R), absorbance (A) and transmittance (T) were obtained from the measured *S*-parameters and EMI shielding due to absorption (SE_A) and reflection (SE_R) were investigated. The mathematical interpretation of SE_A, SE_R and SE_M are [15]

$$SE_A\,(dB) = -10\log(1 - A_{eff}) = -10\log\frac{T}{1-R}$$

$$SE_R(dB) = -10\log(1 - R)$$

$$SE_M(dB) = -20\log(1 - 10^{-SE_A/10})$$

The real and imaginary part of complex permittivity ($\varepsilon^* = \varepsilon' - i\varepsilon''$) was determined from the obtained *S*-parameters by using standard Nicholsion-Ross-Weir (NRW) method.[25]

View Article Online
DOI: 10.1039/C6RA14277J

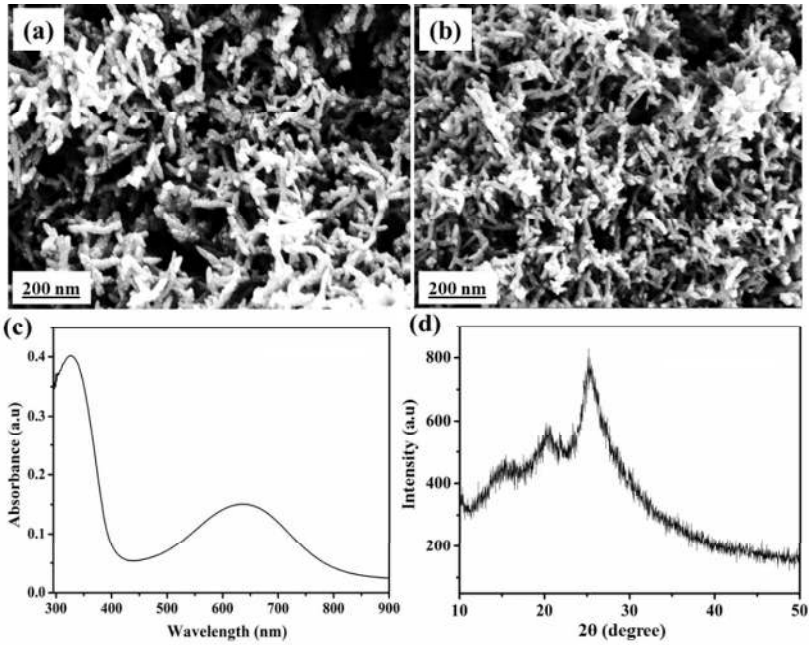

Fig.1. **(a), (b)** surface morphology, **(c)** UV-visible spectra and **(d)** X-ray diffraction pattern of synthesized PANI nanofiberes.

3. Results and discussion

The surface morphology of the as synthesized PANI nanofibers is shown in **Fig. 1(a)** and **Fig. 1(b)**. The diameters of the PANI fibres were found 70-90 nm whilst length was ~ 1 µm. Moreover, a few small agglomerated regions were also observed. The UV-visible spectra of as synthesized PANI nanofibers in N-Methyl-2-pyrrolidone (NMP) is shown in **Fig.1 (c).** The two strong absorption bands obtained at 326 nm and 633 nm correspond to π-π* transition and quinoid ring transition, respectively, in the polyaniline chain and hence implies the interaction in between PANI nanofiber and NMP.[26, 27] Since NMP is a highly polar solvent, in presence of PANI nanofiber, the solute-solvent interactions becomes strong. According to the literature,[27] it results a de-protonation of the polyaniline chain (through hydrogen bonding) and conversion of emaraldine salt (ES) to emaraldine base (EB).[27] The X-ray diffraction pattern of PANI nanofibere is shown in **Fig.1 (d).** The obtained diffractogram suggests the semi crystalline nature of as synthesized PANI nanofiberes.[28] The appearance of three peaks in the diffractogram at 2θ values of 15°, 20° and 25° suggesting the formation conducting PANI nanofiber.[27, 28]

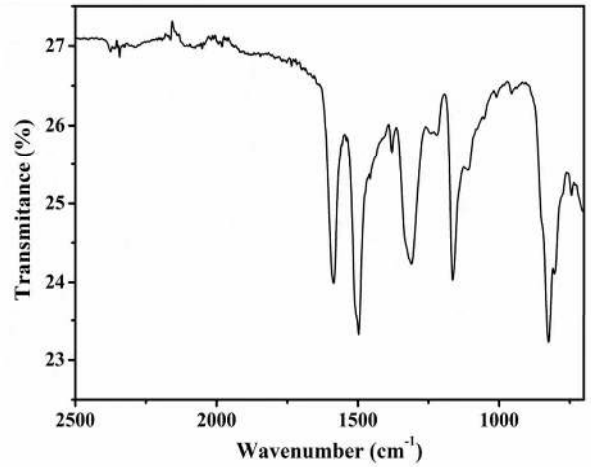

Fig.2. FTIR spectra of synthesized PANI nanofiberes.

The FTIR spectra of synthesized PANI naofiberes is shown in **Fig.2**. As shown in **Fig.2**, the observed peaks at ~1591 cm^{-1} and at ~1495 cm^{-1} represents C=C stretching vibrations of the quinod and benzoid rings respectively.[12] 1400-1000 cm^{-1} is the C-N stretching region for secondary aromatic amines. Most prominent peak is at 1319, representing the C-N stretching for aromatic amines. In the finger print region, the prominent peak at 829 cm^{-1} is thought to arise from C-H out of plane bending modes.[12]

View Article Online
DOI: 10.1039/C6RA14277J

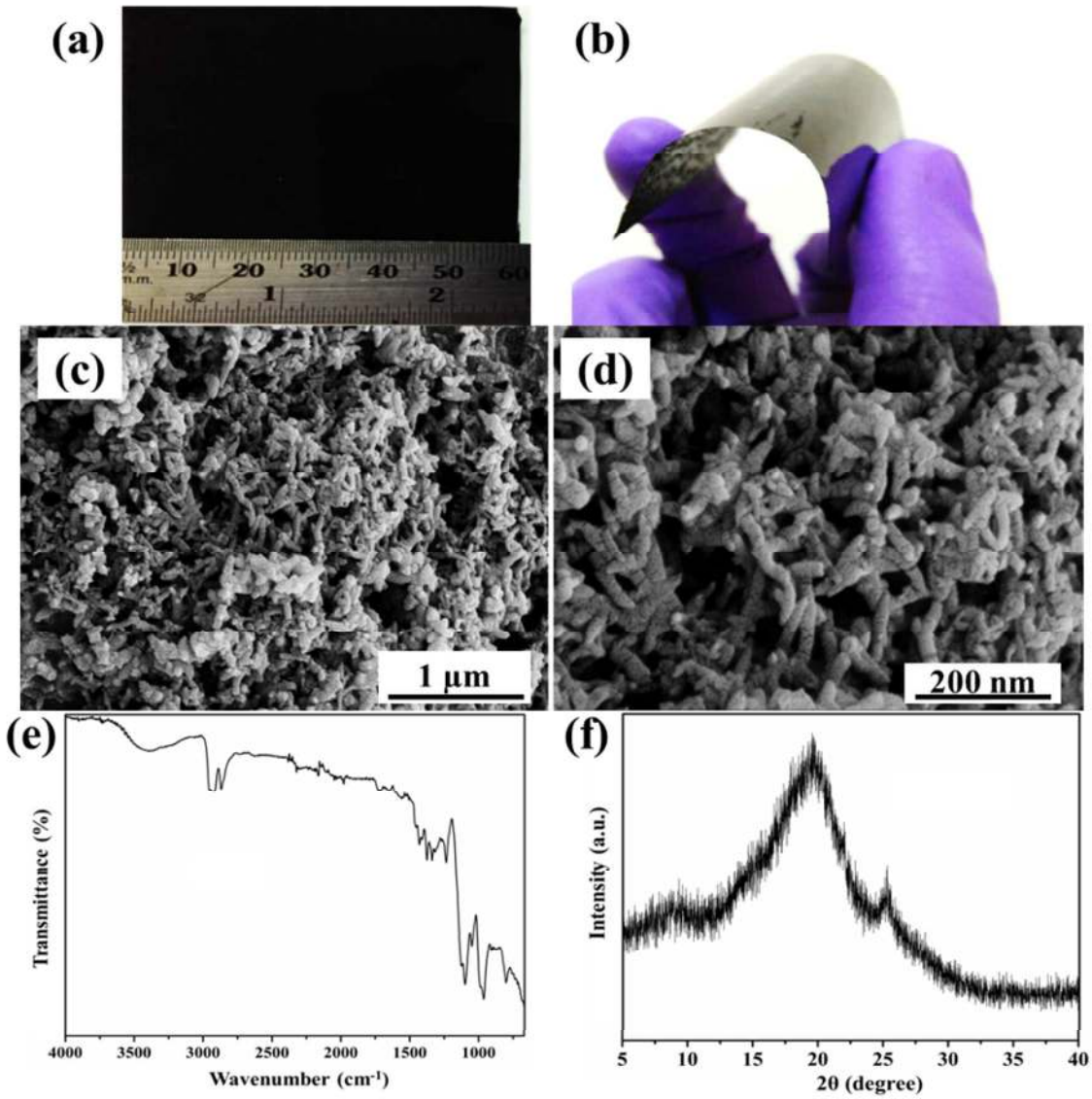

Fig.3. **(a), (b)** Optical images, **(c), (d)** cross-sectional SEM images, **(e)** FTIR spectra and **(f)** XRD pattern of PVBPN film.

View Article Online
DOI: 10.1039/C6RA14277J

Journal Name

ARTICLE

The cross sectional surface morphology, FTIR spectra and XRD pattern of prepared PVBPN nanocomposite film are shown in **Fig.3** along with its optical images. The cross sectional SEM images of PVBPN film (**Fig.3 (b)** and **Fig.3 (c)**) show the distribution of PANI nanofibers in the PVBPN film. It suggests the improvement of loss factor and dielectric loss can takes place along the PANI nanofibers that can enhance EMI SE through absorption. In the FTIR spectra of PVBPN film (**Fig.3 (e)**), the broad peak at ~ 3296 cm^{-1} assigned for OH stretching of the alcohol fragment of PVB. The peaks at ~ 2918 and 2870 corresponds for asymmetric and symmetric CH_2 stretching whereas the peak ~ 1432 cm^{-1} is believed to be due to the CH_2 bending.[21] The peak observed at 1732 cm^{-1} suggests the carbonyl stretching of the acetate fragment of the PVB.[21] **Fig.3 (f)** shows the XRD pattern of PVBPN nanocomposites film, the wide diffraction peak of PVB (2θ ~ 20°) was observed with most prominent PANI nanofiber peak (2θ ~ 25°). Thus it also suggests the presence of PANI nanofibers in the PVBPN film.

The variation of obtained total EMI shielding effectiveness (SE_T), shielding effectiveness due to absorption (SE_A) and shielding effectiveness due to reflection (SE_R) of PVBPN nanocomposites in the X-band (8.2-12.4 GHz) and Ku-band (12.4-18 GHz) frequency range are shown in **Fig.4 (a)** and **Fig.4 (b)** respectively. In the X-band, the average SE_T value was obtained ~ 26 dB (SE_A is ~ 21 dB and SE_R is ~ 5 dB) which was found to increase to ~ 30 dB (SE_A is ~ 26 dB and SE_R is ~ 4 dB) in the Ku-band. Thus it is observed that the EMI SE of PVBPN increases with frequency (8.2-18 GHz) and the EMI shielding due to absorption of this nanocomposite is much higher than EMI shielding due to reflection. The average specific EMI SE of PVBPN film in X-band was obtained ~ 72±2 dB cm^3g^{-1} which was found to be ~ 91±2 dB cm^3g^{-1} for Ku-band. A comparison of EMI shielding property of as prepared sandwiched PVBPN nanocomposites film with recently developed PANI composites under optimized conditions is tabulated in **Table 1**.

The incident electromagnetic wave generates an electric field over the conducting PVBPN surface opposite to applied field as the electron cloud near the surface gets distorted and it passes through the PVBPN nanocomposite by changing its time average power, $P_{av} = \frac{1}{2}\int (E \times H^*) dS$.[31] Due to this the incident electromagnetic waves phase changes and magnitude decreases exponentially.[31] The real part of propagation constant, $\gamma_s = \sqrt{j\omega\mu'\sigma_s}$, ($\omega$ is the angular frequency, $\omega=2\pi f$, μ' is the permeability and σ_s is the shield conductivity, $\sigma_s = \omega\varepsilon_o\varepsilon''$) determines the EMI attenuation due to absorption (EM attenuation constant, α).[7]

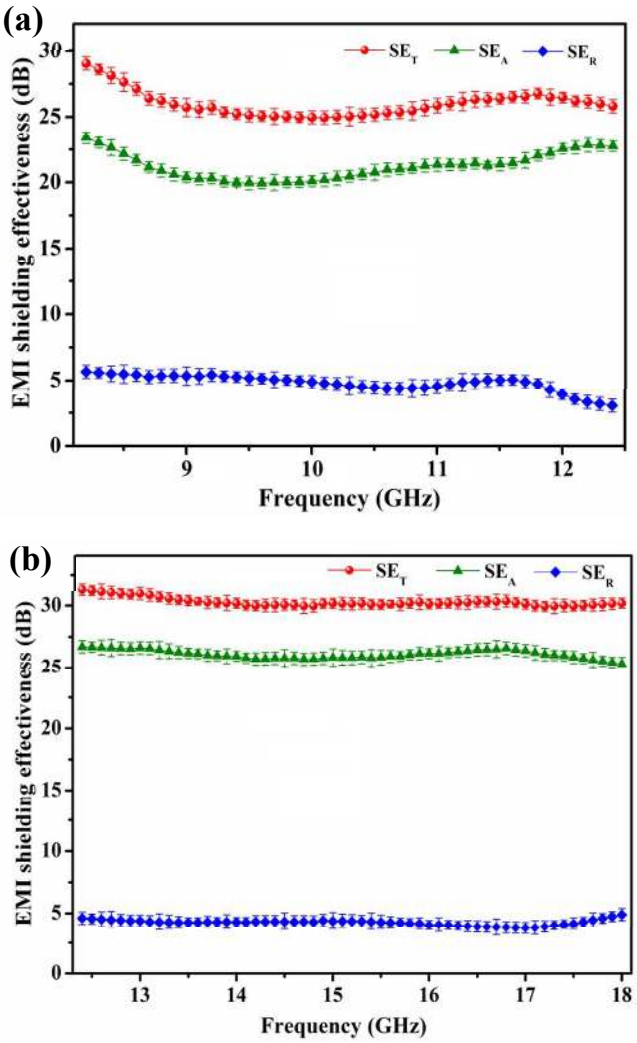

Fig.4. Variation of total EMI shielding effectiveness (SE_T), shielding due to absorption (SE_A) and shielding due to reflection (SE_R) of PVBPN film in the **(a)** X-band (8.2-12.4 GHz) and **(b)** Ku-band (12.4-18 GHz).

View Article Online
DOI: 10.1039/C6RA14277J

Table. 1. A comparison of the average total EMI shielding effectiveness (SE_T), shielding due to absorption (SE_A) and shielding due to reflection (SE_R) of various reported materials with present work under optimal conditions

Material	Frequency	SE_T(dB)	SE_A(dB)	SE_R(dB)	Thickness	Reference
Fe_3O_4@PANI/polyazomethine/ polyetheretherketone	2-18 GHz	~ 10	~ 8	~ 2	2 mm	**29**
SBS-PANI.DBSA	7.8-12.4 GHz	~35	-	-	2 mm	**30**
PANI-CNT/polystyrene	12.4-18 GHz	~ 24	~ 18	~ 6	1 mm	**15**
Polystyrene -PANI-clay	8 GHz	16.2	-	-	1 mm	**14**
PU-PANI	8-12 GHz	~ 10	-	-	1.9 mm	**13**
PVB-PANI nanofiber	**8.2-12.4 GHz**	**~ 26**	**~ 21**	**~ 5**		**Present work**
	12.4-18 GHz	**~ 30**	**~ 26**	**~ 4**	**0.78±0.02 mm**	**Present work**

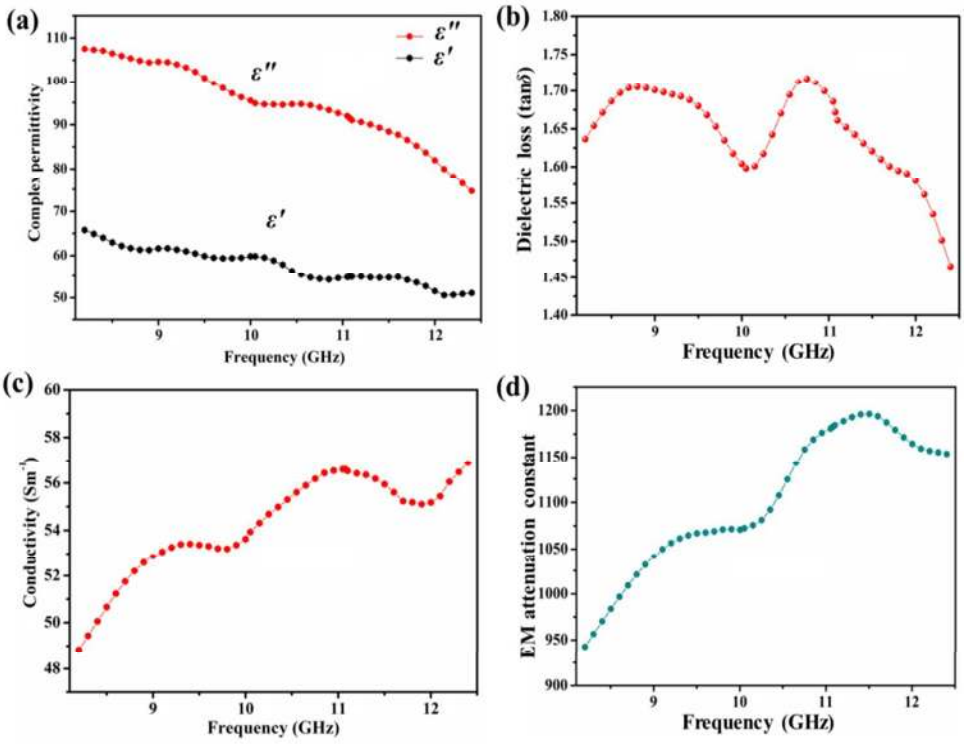

Fig.5. Variation of **(a)** real and imaginary part of complex permittivity, **(b)** dielectric loss, **(c)** shield conductivity and **(d)** EM attenuation constant of PVBPN film in the X-band.

The distance required for the electromagnetic wave to be attenuated to 1/e of its initial amplitude is known as skin depth or penetration depth (δ_s),[3, 7] mathematically, $\delta_s = \sqrt{2/\mu'\omega\sigma_s}$. For electrically thick shielding materials,[31, 7, 32]

$$SE_R(dB) = -10\log\left\{\frac{(1-R)}{16\omega\varepsilon_o\mu'}\right\}$$

$$SE_A(dB) = -20\frac{t}{\delta_s}\log e = -8.68t\left(\frac{\sigma_s\omega\mu'}{2}\right)^{\frac{1}{2}}$$

$$\alpha = \frac{\sqrt{2}\pi f}{c} \times \left[(\mu''\varepsilon'' - \mu'\varepsilon') + \{(\mu''\varepsilon'' - \mu'\varepsilon')^2 + (\mu'\varepsilon'' - \mu''\varepsilon')^2\}^{\frac{1}{2}}\right]^{\frac{1}{2}}.$$

View Article Online
DOI: 10.1039/C6RA14277J

Journal Name

ARTICLE

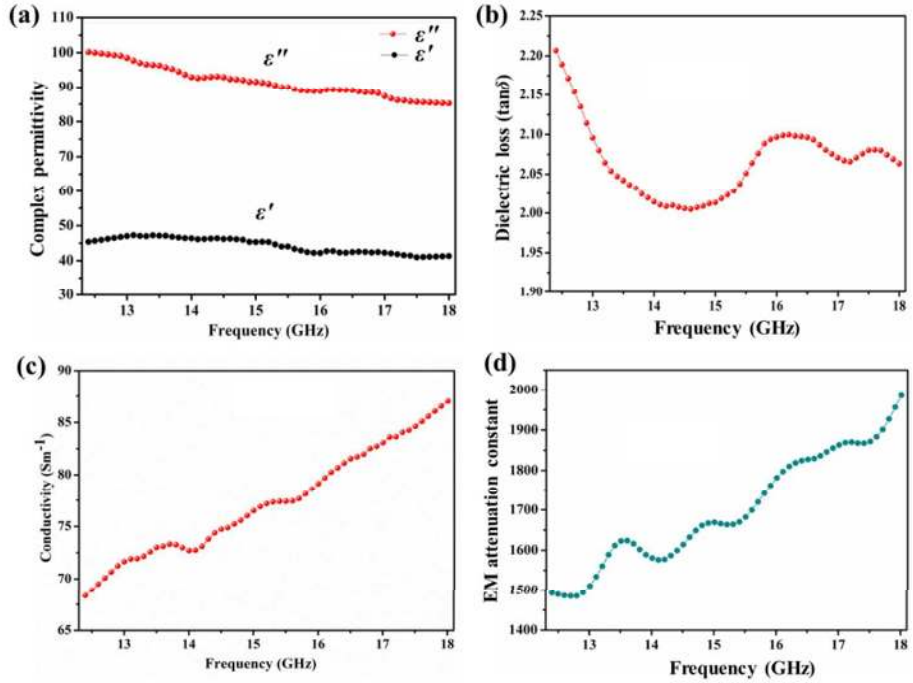

Fig.6. Variation of **(a)** real and imaginary part of complex permittivity, **(b)** dielectric loss, **(c)** shield conductivity and **(d)** EM attenuation constant of PVBPN film in the Ku-band.

The variation of real and imaginary part of complex permittivity ($\varepsilon^* = \varepsilon' - i\varepsilon''$) of the PVBPN film in the X-band is shown in **Fig.5 (a)** along with dielectric loss tangent ($tan\delta = {\varepsilon''}/{\varepsilon'}$, **Fig.5 (b)**), shield conductivity (**Fig.5 (c)**) and EM attenuation constant (**Fig.5 (d)**). The real part of complex permittivity (ε') corresponds to the amount of polarization occurred inside the shield material and imaginary part (ε'') corresponds to the dissipation of electrical energy.[7, 32] It was observed that, both ε' and ε'' decreases with frequency due to the decrease of interfacial polarization and heterogeneity of PVB and PANI nanofiberes.[3, 7] The shield conductivity of PVBPN film was 49-58 Sm^{-1} and the EM attenuation constant was 950-1170. In case of Ku-band, the shield conductivity increases to 67-87 Sm^{-1} (**Fig.6 (c)**) with high dielectric loss tangent (**Fig.6 (b)**). The enhancement of conductivity of PVBPN film with frequency is due to the increased orderness and compactness of the PANI nanofibers in the PVB matrix. The variation of EM attenuation constant of PVBPN film in the Ku-band is shown in **Fig.6 (d).** Compared to X-band, the EM attenuation constant of PVBPN film in the Ku-band is high (1500-1980). Thus, it suggests the excellent EMI shielding due to absorption property of PVBPN film with frequency. The calculated penetration depth (δ_s) of PVBPN film in the X-band and Ku-band is shown in **Fig.7 (a)** and **Fig.7.(b)** respectively. As shown in **Fig.7 (a),** the penetration depth of PVBPN film exponentially decreases from ~ 0.77 mm to ~ 0.61 mm in X-band. Similarly, in Ku-band it decreases from ~ 0.53 mm to ~ 0.4 mm. Thus, the decrease of penetration depth of PVBPN film with frequency also results in enhancement of EMI shielding due to absorption. Each PANI nanofiber in the composite is surrounded by the effective medium. Hence, the attenuation of incident electromagnetic radiation also takes place due to the scattering.

View Article Online
DOI: 10.1039/C6RA14277J

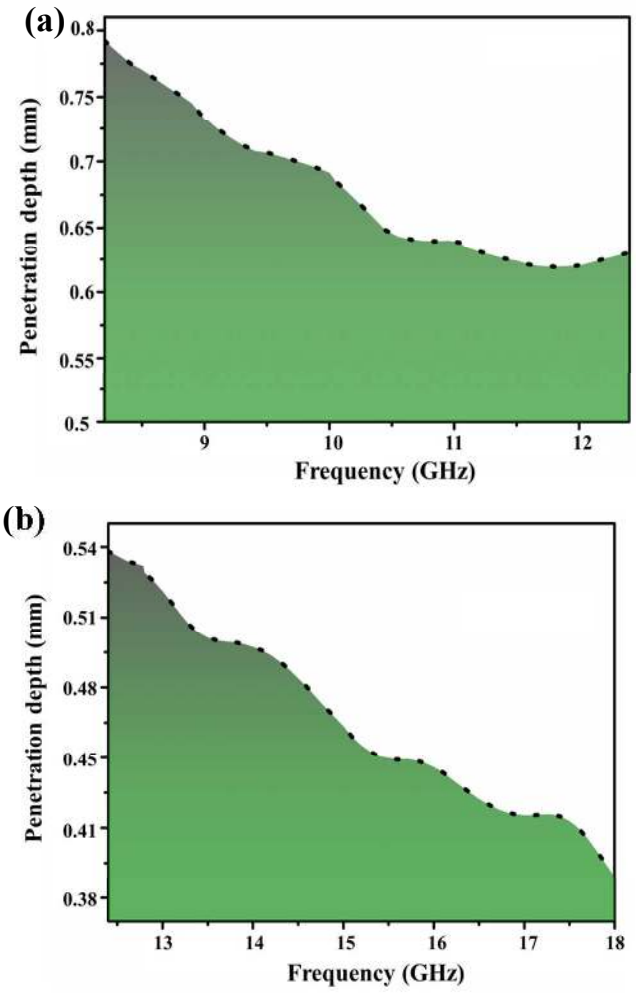

Fig.7. Variation of penetration depth of PVBPN film in the **(a)** X-band and **(b)** Ku-band frequency.

The scattering attenuation depends on number of particles (nanofiberes) in a volume in the effective medium.[33] The equation of scattering attenuation (I_{sc}) is [33, 34]

$$I_{sc} = I_0 \exp\left\{-n\frac{k^4(|\varepsilon_{r1}-1|^2+|\mu_{r1}-1|^2)}{6\pi}\delta_s\right\}$$

Where, k is the wave number, n is the number of particles per unit volume of the composite. ε_{r1} and μ_{r1} corresponds to the relative permittivity and permeability of the material respectively. Since the present system contains disordered PANI nanofibers, therefore expected I_{sc} is also more and thus it is helping in enhancement of EMI shielding as the electromagnetic attenuation by a small particle (I_T) is equal to the absorption attenuation of refracted wave (I_{ab}) and I_{sc} i.e. $I_T = I_{ab} + I_{sc}$.[33, 34] Apart from the above discussions, high dielectric loss PANI nanofibers creates some discontinuous networks in the composite which leads to the EM energy attenuation through antenna mechanism (PANI nanofiberes acts like a receiving antenna which receives incident electromagnetic radiation and converts it to micro current) and results high EMI shielding due to absorption.[16] Since, PANI nanofiberes are distributed randomly, there is a chance of huge counteract ion of incident EM radiation and due to that incident electromagnetic energy transforms into dissipation current which value decreases exponentially with propagation due to the interfacial electric polarization and dielectric loss of PVBPN film.

4. Conclusion

The PANI nanofibers were successfully synthesized at -30±2 °C. Investigated EMI shielding property of optimally prepared PVB-polyaniline nanofiber composite (PVBPN) flexible film shows an outstanding EMI shielding effectiveness for X-band and Ku-band frequency range with an appreciable film thickness. The 0.78±0.02 mm thicker sandwiched PVBPN film shows ~ 26 dB and ~30 dB EMI shielding effectiveness for X-band and Ku-band respectively. Mechanistically, EMI shielding due to absorption was found to be dominant for each band. Furthermore, enhancement of conductivity, dielectric loss and EM attenuation constant with frequency conceive excellent EMI shielding due to absorption of PVBPN film.

Acknowledgments

Authors gratefully acknowledge the prof. K. J Vinoy, Dept. of Electrical and Communication Engineering, IISc, India for his help during the EMI shielding, dielectric measurements and some valuable discussions. This work is financially supported by Department of Science and Technology SB/S3/ME/51/2012 and technically supported by IISc advanced characterization centre and CeNSE.

References

1 M. H. Al-Saleh, W. H. Saadeh and U. Sundararaj, *Carbon*, 2013, **60**, 146–156.

2 J. Li, G. Zhang, Z. Ma, X. Fan, X. Fan, J. Qin and X. Shi, *Compos. Sci. Technol.*, 2016, **129**, 70–78.

3 X. C. Tong, *Advanced Materials and Design for Electromagnetic Interference Shielding*, CRC Press, 2008.

4 M. Arjmand, A. A. Moud, Y. Li and U. Sundararaj, *RSC Adv.*, 2015, **5**, 56590–56598.

View Article Online
DOI: 10.1039/C6RA14277J

5 Y. Zhang, Z. Wang, B. Zhang, G.-L. Zhao and S. M. Guo, *RSC Adv.*, 2015, **5**, 93499–93506.

6 M. H. Al-Saleh and U. Sundararaj, *Carbon*, 2009, **47**, 1738–1746.

7 J. W. Gooch and J. K. Daher, *Electromagnetic Shielding and Corrosion Protection for Aerospace Vehicles*, Springer New York, New York, NY, 2007.

8 Z. Chen, C. Xu, C. Ma, W. Ren and H.-M. Cheng, *Adv. Mater.*, 2013, **25**, 1296–1300.

9 J. Joo and A. J. Epstein, *Appl. Phys. Lett.*, 1994, **65**, 2278–2280.

10 H. S. Nalwa, *Handbook of Organic Conductive Molecules and Polymers, Charge-Transfer Salts, Fullerenes and Photoconductors*, Wiley, 1997.

11 P. Saini, V. Choudhary, N. Vijayan and R. K. Kotnala, *J. Phys. Chem. C*, 2012, **116**, 13403–13412.

12 P. C. Ramamurthy, A. N. Mallya, A. Joseph, W. R. Harrell and R. V. Gregory, *Polym. Eng. Sci.*, 2012, **52**, 1821–1830.

13 K. Lakshmi, H. John, K. T. Mathew, R. Joseph and K. E. George, *Acta Mater.*, 2009, **57**, 371–375.

14 J. D. Sudha, S. Sivakala, K. Patel and P. Radhakrishnan Nair, *Compos. Part Appl. Sci. Manuf.*, 2010, **41**, 1647–1652.

15 P. Saini, V. Choudhary, B. P. Singh, R. B. Mathur and S. K. Dhawan, *Synth. Met.*, 2011, **161**, 1522–1526.

16 R. F. Zhuo, L. Qiao, H. T. Feng, J. T. Chen, D. Yan, Z. G. Wu and P. X. Yan, *J. Appl. Phys.*, 2008, **104**, 94101.

17 A. Kumar, S. Banerjee, J. P. Saikia and B. K. Konwar, *Nanotechnology*, 2010, **21**, 175102.

18 J. Huang, S. Virji, B. H. Weiller and R. B. Kaner, *J. Am. Chem. Soc.*, 2003, **125**, 314–315.

19 N. Joseph, J. Varghese and M. T. Sebastian, *RSC Adv.*, 2015, **5**, 20459–20466.

20 C. Nath, A. Kumar, K.-Z. Syu and Y.-K. Kuo, *Appl. Phys. Lett.*, 2013, **103**, 121905.

21 A. S. Roy, S. Gupta, S. Seethamraju, G. Madras and P. C. Ramamurthy, *Compos. Part B Eng.*, 2014, **58**, 134–139.

22 S. Gupta, S. Seethamraju, P. C. Ramamurthy and G. Madras, *Ind. Eng. Chem. Res.*, 2013, **52**, 4383–4394.

23 J. Huang and R. B. Kaner, *J. Am. Chem. Soc.*, 2004, **126**, 851–855.

24 Y. Yang, M. C. Gupta, K. L. Dudley and R. W. Lawrence, *Nano Lett.*, 2005, **5**, 2131–2134.

25 L. F. Chen, C. K. Ong, C. P. Neo, V. V. Varadan and V. K. Varadan, *Microwave Electronics: Measurement and Materials Characterization*, John Wiley & Sons, 2004.

26 J. G. Masters, Y. Sun, A. G. MacDiarmid and A. J. Epstein, *Synth. Met.*, 1991, **41**, 715–718.

27 A. Rahy and D. J. Yang, *Mater. Lett.*, 2008, **62**, 4311–4314.

28 K. Lee, S. Cho, S. Heum Park, A. J. Heeger, C.-W. Lee and S.-H. Lee, *Nature*, 2006, **441**, 65–68.

29 W. Wei, X. Yue, Y. Zhou, Y. Wang, Z. Chen, M. Zhu, J. Fang and Z. Jiang, *RSC Adv.*, 2014, **4**, 11159–11167.

30 M. Magioli, B. G. Soares, A. S. Sirqueira, M. Rahaman and D. Khastgir, *J. Appl. Polym. Sci.*, 2012, **125**, 1476–1485.

31 C. A. Grimes and D. M. Grimes, in *, 1993 IEEE Aerospace Applications Conference, 1993. Digest*, 1993, pp. 217–226.

32 Y. Zhang, Z. Wang, B. Zhang, C. Zhou, G.-L. Zhao, J. Jiang and S. M. Guo, *J. Mater. Chem. C*, 2015, **3**, 9684–9694.

33 C. F. Bohren and D. R. Huffman, *Absorption and Scattering of Light by Small Particles*, John Wiley & Sons, 2008.

34 H. Guan, J. Xie, G. Chen and Y. Wang, *Mater. Chem. Phys.*, 2014, **143**, 1061–1068.